Evaluation of CO_2 and Nd:YAG lasers for the selective laser sintering of HAPEX®

M M Savalani*, L Hao, and **R A Harris**
Rapid Manufacturing Research Group, Loughborough University, Loughborough, UK

The manuscript was received on 30 June 2005 and was accepted after revision for publication on 27 September 2005.

DOI: 10.1243/095440505X32986

Abstract: This paper evaluates and compares the performance of a CO_2 and Nd:YAG laser for the selective laser sintering (SLS) of a commercial hydroxyapatite reinforced polyethylene (HA-HDPE) bioactive ceramic polymer composite material. Single-line and layer specimens were produced to compare the effects of different lasers on the material sintering. It was found that the processing window was much larger for the CO_2 laser as compared to the Nd:YAG laser. Furthermore, the Nd:YAG processing window was highly dependent on the pulse width and pulse repetition rate parameter settings. Furthermore, the processing windows for both the laser systems were affected by the particle size of the HA-HDPE powders. The degree and mechanism of particle fusion existing in the composites layers were greatly influenced by the laser source and particle size. The results presented in this work clearly indicate that the CO_2 laser would present a better performance than the Nd:YAG laser for the SLS of HAPEX® in terms of operation range, speed, processing efficiency, and, subsequently, greater potential as an SLS processing method for bioactive implant products.

Keywords: laser, selective laser sintering, hydroxyapatite, polyethylene, bioactive implants

1 INTRODUCTION

Selective laser sintering (SLS) is a layer manufacturing or solid freeform fabrication technique, which generates complex three-dimensional parts by solidifying successive layers of powder material on top of each other. Solidification is obtained by fusing or sintering selected areas of the successive powder layers using thermal energy supplied through a laser beam. The selected area corresponds to a cross-section of the part as calculated from a computer-aided design (CAD) model. One of the major advantages associated with SLS technology is material versatility compared to other rapid prototyping/rapid manufacturing (RP/RM) techniques, while manufacturing complex and customized geometries rapidly [**1**, **2**]. Thus far, a wide range of materials including metals, ceramics, polymers, and composites (polymer/ceramic, multiphase metal) have been investigated by employing SLS, directly or indirectly. The focus of recent research has been geared towards direct SLS. SLS has the ability to produce end products directly and automatically from a three-dimensional computer model representation, such as that from CT or MRI scans. This technique demonstrated some ability directly to fabricate customized implants for solid and porous bone replacement and implants of controlled porosity for use as tissue scaffolds [**3**].

Among the various available industrial lasers, CO_2 and Nd:YAG lasers are the two most investigated lasers for SLS. To fabricate quality parts using direct SLS, the process mechanics relative to the interaction between the laser beam and powder material is critical and one of the dominant phenomena that defines the feasibility and quality of any SLS process [**4**]. It is well known that the type of laser beam affects the final properties (i.e. mechanical properties, physical density, and surface texture) of the final part [**5**]. Hence, the choice of laser is not independent of the material that has to be sintered as different lasers would have a varied effect on the same material [**6**]. Some of the major differences among the various laser systems include: wavelength, coherence, mode of operation, and beam diameter.

**Corresponding author: Wolfson School of Mechanical and Manufacturing Engineering, Loughborough University, Loughborough, Leicestershire LE11 3TU, UK. email: m.m.savalani@lboro.ac.uk*

Optimally, the laser wavelength should be adapted to the powder material to be sintered since laser absorption greatly changes with the material and repetition rate or wavelength of the laser light. CO_2 lasers have a wavelength of 10.6 μm and are well suited for sintering various polymers and ceramic oxide powders such as nylons, polymethylacrylate (PMMA), polytetrafluoroethylene (PTFE), and zinc oxide [**7**] as polymers and oxide ceramics depict high adsorption at far infrared or long wavelength.

Nd:YAG lasers have an active medium of neodymium in a yttrium aluminium garnet (YAG). These lasers have short wavelengths of 1.06 μm, which may outperform CO_2 lasers for metallic materials that absorb much better at short wavelength. Nd:YAG lasers are favourable for sintering carbide ceramics owing to lower reflectivity and higher surface adsorption [**7**, **8**]. The feasibility study of SLS by Vaucher *et al.* [**9**] investigated the Nd:YAG laser sintering of metal and ceramic composites including aluminium alloy/silicon carbide, titanium/silicon carbide, and titanium/graphite and single layers and multilayers of metal/ceramic composites were successfully produced. Nd:YAG laser was also used in SLS processing of crystalline low-purity alumina and ammonium dihydrogen phosphate powder blends. It was observed that ammonium dihydrogen phosphate phase melted and wet the alumina in the processing [**10**]. Alexandre *et al.* [**11**] used a Nd:YAG laser for SLS to produce three-dimensional porous parts from ceramic powders and preceramic polymers and found promising microstructure in the resulting composite. In this approach, selective laser processing of a polysiloxane preceramic polymer serves to bind the ceramic grains together by decomposing the polymer during laser heating scans.

Although a great deal of work has been conducted on sintering single-component powders and material mixtures using the CO_2 or Nd:YAG laser, relatively little work has been conducted to investigate the comparative effects of both CO_2 and Nd:YAG laser. Kruth *et al.* compared the performance of the CO_2 and Nd:YAG laser in SLS of several different steel–copper powder mixtures and found that the Nd:YAG laser gives better results than the CO_2 laser for direct liquid phase sintering of steel–copper parts [**12**]. Recently, SLS has been used to investigate the direct fabrication of bone replacement substitutes on a commercial SLS system using a CO_2 laser to sinter polymer and ceramic mixtures, including PEEK/HA and PVA/HA [**13**, **14**]. Thus far, no work has been done on investigating the performance of both the CO_2 and Nd:YAG laser to sinter polymer ceramic compounded composite materials. Furthermore, it would be interesting to compare the sintering of composites with high ceramics content ratio using both the CO_2 and Nd:YAG laser.

The objective of the study described in this paper was to investigate comparatively the feasibility and process characteristics of using both a CO_2 and Nd:YAG laser sintering of a hydroxyapatite (HA) particulate reinforced high-density polyethylene (HDPE) composite (HA-HDPE) developed by Bonfield and co-workers [**15**, **16**] which has been used clinically as bone replacement substitute for over 15 years [**17**]. This clinically used grade of HA-HDPE composite is known commercially as HAPEX®. The mechanisms behind the differences in the sintering and performance of HA-HDPE when sintered by CO_2 and Nd:YAG laser were analysed and elucidated.

2 METHODOLOGY

2.1 Material and preparation

The commercial HAPEX® grade containing 40 per cent volume ratio of synthetic HA is used in this study. This grade was chosen for its known biocompatibility and bioactivity [**18**]. The comprising raw materials used in HAPEX® are HDPE pellets (Rigidex HM4560XP) by BP Chemicals Ltd and synthetic HA particles (P218R) supplied by Plasma Biotal Ltd. The HA particles had a median size ($d_{0.5}$) of 3.80 μm and a specific surface area of 13.54 m^2/g^{-1}, while the theoretical density was 3160 kg/m^{-3}. These materials were blended and subsequently compounded in a twin-screw extruder (Betol BTS40L, Betol, Luton, UK) to produce the HA-HDPE composite. The extruded composites were subsequently pelletized in a Betol pelletizer and powderized in an ultra-centrifugal mill (Retsh powderizer) using a 1 mm, 500 μm, and 250 μm aperture size sieve, consecutively. Detailed description of the fabrication technique is described in the work by Wang *et al.* [**19**].

The resultant particles were then sieved at various sizes to include below 75 μm, 75–106 μm, 106–150 μm, and 150–212 μm by a sieve shaker (Endecotts Ltd). Sieves of aperture sizes 75, 106, 150, 212, and 250 μm were stacked from smallest to largest. The stacked sieves vibrated and rotated to achieve even and well-distributed sieving. To remove any electrostatic effects the sieve shaker was earth. Particles were vibrated for a period of 15 min to maximize uniformity. Particle size distribution was analysed using a Mastersize S particle size analyser (Malvern Instruments Ltd).

2.2 Experimental processing

CO_2 and Nd:YAG laser systems were set-up to investigate the SLS of HAPEX®. A GSI Lumonics JK701H

Nd:YAG (wavelength 1.06 μm) pulsed laser with a maximum power of 550 W was used. The focused beam diameter was measured at 800 μm. The scanning speed of the laser beam could be varied from 0.2 to 83 mm/s in increments of 0.02 mm/s. Available pulse duration varied from 0.5 to 20 ms and the repetition rate varied up to 100 Hz. The working environment was in an inert gas shroud (Ar) with a minimum pressure of 2 bar in order to minimize possible surface oxidation. A Synrad 48-1-28 CO_2 (wavelength 10.6 μm) continuous laser with a maximum power of 10 W was used. The scanning speed of the laser beam varies from 0.2 to 10 000 mm/s. The laser beam was focused to 200 μm at a focal length of 241 mm. The main characteristics of the CO_2 laser are the controllable output, long operating life, good beam quality, and easy maintenance.

Powders were sintered in a custom aluminium sintering cell. The cell was an aluminium block that had four regular square-shaped pockets of dimensions 10×10 mm. Powders were loaded into the cell by a spatula. The volume was overfilled and excess powder was removed by scraping the top surface with an aluminium sheet.

The approach taken in this work was initially to build single lines of 200 mm length to identify the most appropriate processing conditions for HAPEX® with each laser type. One common parameter, known as specific energy density, was then selected to sinter 6.3×5.6 mm single-layer specimens to compare the effects of both the lasers.

Specific energy density describes the distribution of laser energy in a scanned area along a linear movement and is defined by dividing laser power by velocity and the beam diameter

$$\text{Specific energy density } (\text{W/mm}^2) = \frac{\text{power (W)}}{\text{velocity (mm)} \times \text{spot size (mm)}} \quad (1)$$

Peak power is the amount of energy delivered onto a surface for a given pulse duration

$$\text{Peak power} = \frac{\text{energy (J)}}{\text{pulse duration (ms)}} \quad (2)$$

The velocity and the pulse repetition rate characterize and determine the overlap between consecutive pulses. As the repetition rate increases, the overlap between pulses increases

$$\text{Velocity (mm/s)} = (1 - \text{overlap}(\%)) \times \text{spot size (mm)} \times \text{repetition rate (Hz)} \quad (3)$$

The single-layer specimens were built to provide information with regard to geometry, density, and the particle binding. Various factors need to be considered when the sintering process moves from a single line to a layer, i.e. scan spacing for overlapping beads and scan strategy. In order to compare specimens made from lasers of different spot size, the overlap ratio was kept constant to emulate similar sintering conditions. The overlap ratio was calculated by equations illustrated in Fig. 1. For this study, an overlap ratio of 67.2 per cent was used for both the CO_2 and the Nd:YAG laser. To equate the same amount of overlap ratio

$$\frac{\text{CO}_{2\text{spotsize}}}{\text{CO}_{2\text{scanspacing}}} = \frac{\text{Nd:YAG}_{\text{spotsize}}}{\text{Nd:YAG}_{\text{scanspacing}}} \quad (4)$$

where spot size of the focused CO_2 laser beam was 193 μm, spot size of the focused Nd:YAG was 800 μm and scan spacing applied on the CO_2 laser was 63.3 μm. Hence, the scan spacing applied on the Nd:YAG laser was set at 262 μm.

2.3 Examination

The morphologies of the specimens were examined with a LEO 440 scanning electron microscope

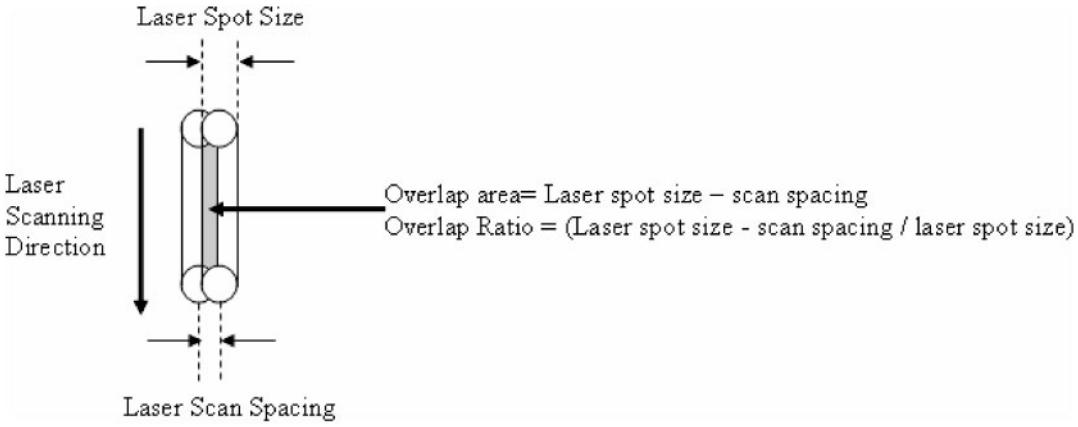

Fig. 1 Illustration of laser scanning and overlap ratio

(SEM) at operating voltages below 20 kV. Such low voltages were chosen to minimize charging and heat damage to the samples. The raw HDPE-HA composite powders and single-layer specimens sintered by CO_2 and Nd:YAG laser were examined. All samples were sputter coated with gold to avoid charging.

2.4 Characterization

The distribution of HA within the HDPE matrix was confirmed by taking SEM images of a cross-section of semi-molten HAPEX® in a furnace at 160 °C for approximately 20 min from ambient temperature. The ash test for HAPEX® involves the burning of HDPE and treating the HA residue at a high temperature (i.e. 650 °C) until constant mass is reached. The ash content of powders was measured, based on the principles of ISO 3451-4 to determine the amount of HA present in the HDPE matrix composite after material sieving. The sintering depth of sintered single-layer specimens was measured by a shadowgraph (Isoma Ltd). The weight of the sintered single-layer specimens was measured using a balance. The mean value of measurements of three specimens for each parameter was recorded for both the sintering depth and weight of specimen. These values were used to calculate the true density.

3 RESULTS AND DISCUSSION

3.1 Microscopic examination and ash test of HAPEX®

Figures 2(a), (b), and (c) illustrate unsintered HAPEX® composite particles of various particle sizes ranging from <75 μm, 75–106 μm, and 106–150 μm. It was observed that most particles were of irregular shape because the powders were generated by mechanical impact in brittle state. Some elongated filaments were present among the particles. There was no considerable difference in the shape according to particle size range. Figures 3(a), (b), and (c) illustrate the unsintered particle size distribution of the materials sieved using the various sieve mesh sizes. It was clear that only approximately 50 per cent of the particles were truly below the size of the sieve. Others were larger, possibly due to particles possessing an elongated morphology in a single direction that may have allowed them still to pass through the sieve apertures. Figure 4 illustrates the presence of HA particles within the HDPE matrix. The HA particles are in the size range of 3–10 μm as specified by the manufacturer and are supposed to be represented by the lighter colour in the microscopy image. From this it is clear that the HA particles are generally

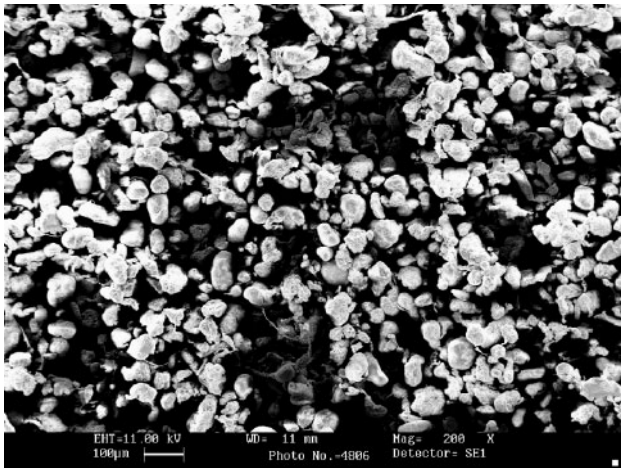

(a)

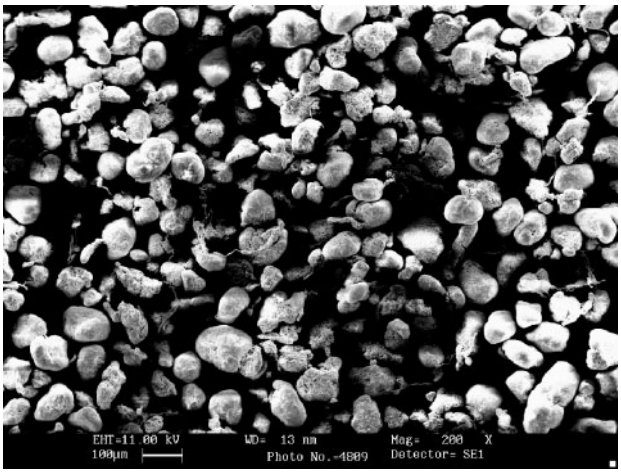

(b)

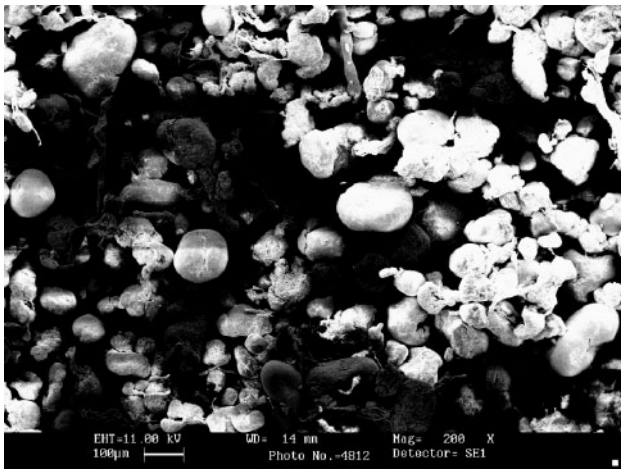

(c)

Fig. 2 SEM micrograph of HAPEX® powders with particle size (a) <75 μm; (b) 75–106 μm; (c) 106–150 μm

well distributed in the HDPE matrix. Table 1 illustrates that 69 per cent ash is obtained following the ash test for the unsieved 40 per cent HA volume ratio commercial HA-HDPE. A maximum variation

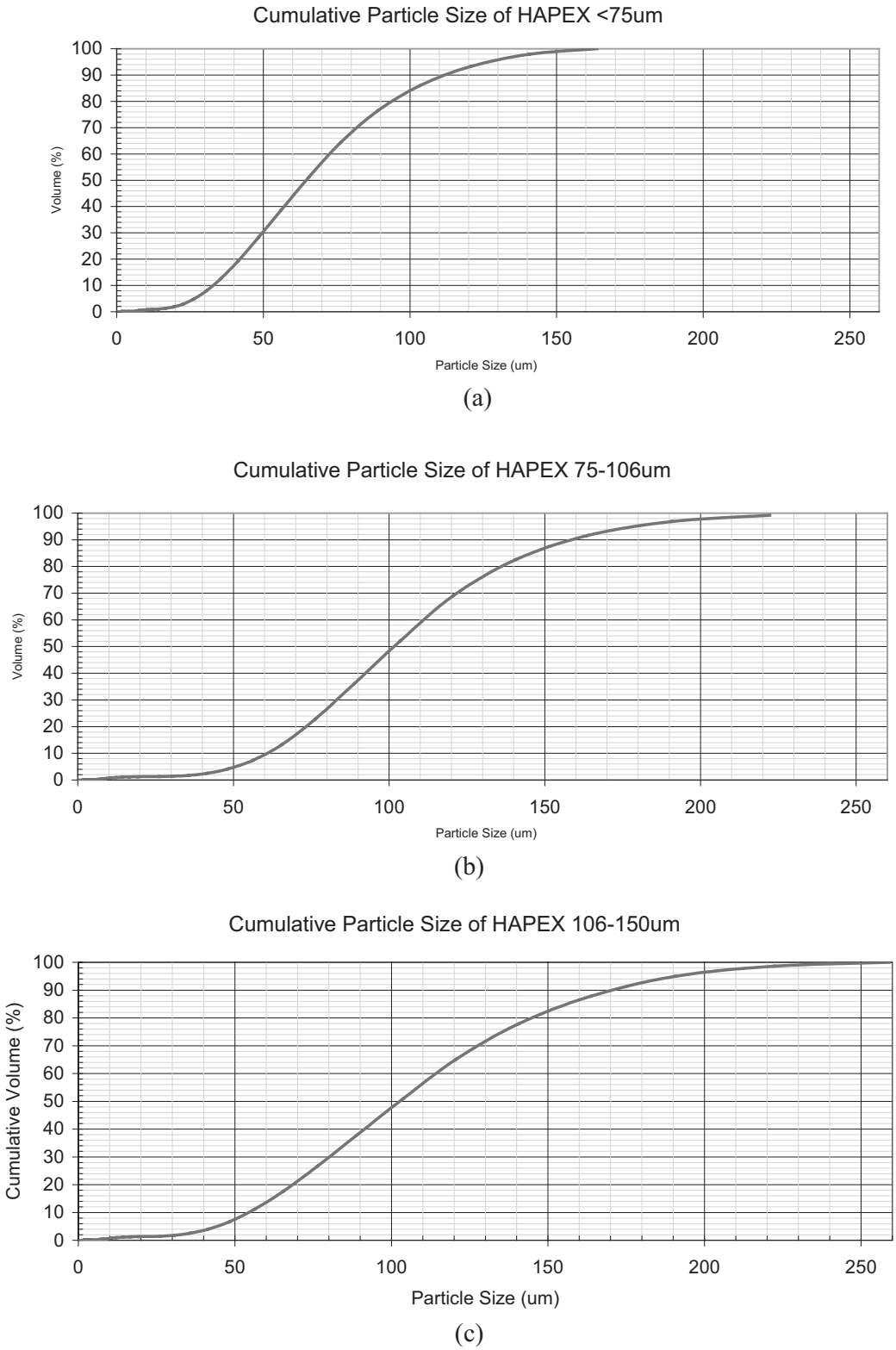

Fig. 3 Cumulative size distribution of HAPEX® powders with particle size (a) <75 μm; (b) 75–106 μm; (c) 106–150 μm

of 2.1 per cent is observed among the sieved HA-HDPE composite compared to the unsieved commercial HA-HDPE. This is minor and considered insignificant.

3.2 Processing window for the CO_2 and Nd:YAG laser

Laser beam power and scan speed determine the amount of energy imparted to the part bed in the

SLS process and are directly related to specific energy density [**5**]. Laser power determines the amount of energy irradiated onto the part bed surface during the scanning of a part section profile. The amount of energy absorbed is determined by the duration of radiation on a unit area. Higher scan speeds result in a reduced amount of energy absorbed per unit area; lower scan speeds have the opposite effect. Since energy density is a function of both laser beam power and scan speed, the processing window was determined experimentally for both lasers by varying laser beam power, *P*, and scan speed, *V*. Samples sintered, by CO_2 and Nd:YAG lasers were typically divided by visual investigation and physical handling into three categories: charred/evaporated, sintered, and those too fragile to handle. The processing window includes laser parameters to generate single-line specimens of HAPEX® with acceptable strength to be handled and being not seriously charred. As is evidenced from Figs 5 and 6, CO_2 laser has a much larger processing window (large range of laser power and scanning speed) to generate sintered HAPEX® specimens than the Nd:YAG laser. The large operation window for CO_2 laser allows a wide variation of the processing parameters and may enforce good process controllability and reliability.

Table 1 HA–HDPE weight ratio at various particle sizes

Particle size	Ash (%)
Un-sieved commercial HA-HDPE	69
<75 μm	66.9
75–106 μm	68.2
106–150 μm	67.35
150–212 μm	67.37

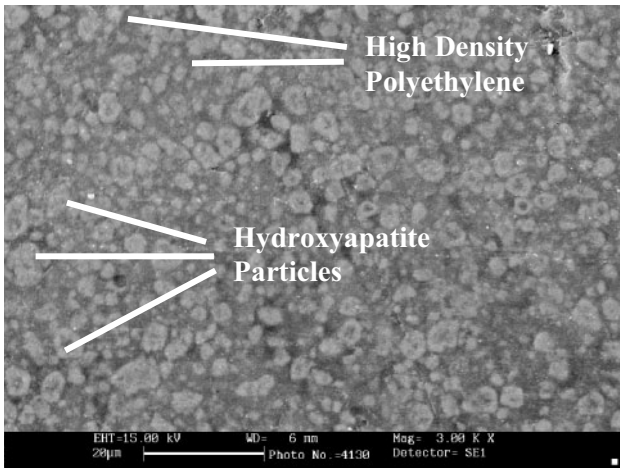

Fig. 4 SEM micrograph of HA particle distribution in HDPE matrix

3.2.1 *CO_2 processing window*

The CO_2 laser was operated in a continuous mode. Figure 5 illustrates that there is a large range of laser power and scanning speed in the processing window for CO_2 laser sintering of acceptable single-line specimens. The acceptable sintering of HAPEX® takes place between energy density values of 0.01 and 0.02 J/mm^2. When the energy density values were below 0.01 J/mm^2, the single-line specimens could not be sintered or were too fragile to handle. On the other hand, when the energy density values were higher than 0.02 J/mm^2, the single-line specimens became dark brown, possibly due to charring of the material.

3.2.2 *Nd:YAG processing window*

Unlike a continuous laser, the laser power of a pulsed laser is a product of the repetition rate (Hz) and pulse energy, where the latter variable is a function of the pulse width. To obtain the best possible processing window for HAPEX® three parameter

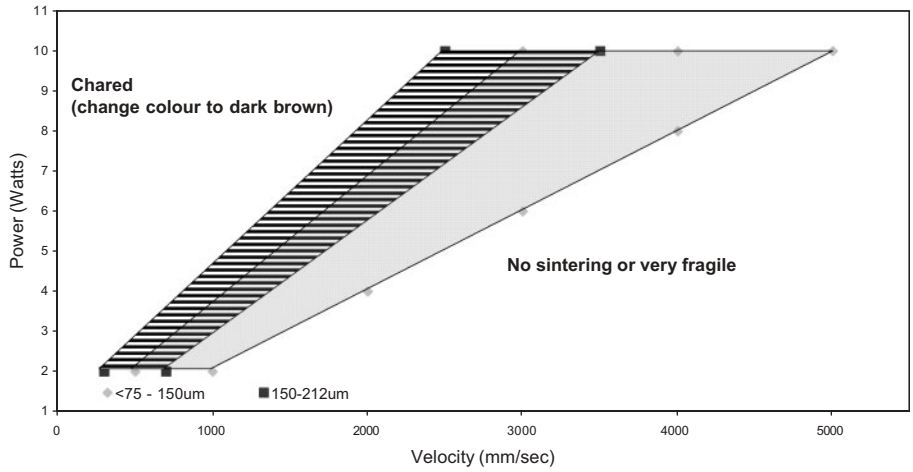

Fig. 5 Processing window using a CO_2 laser

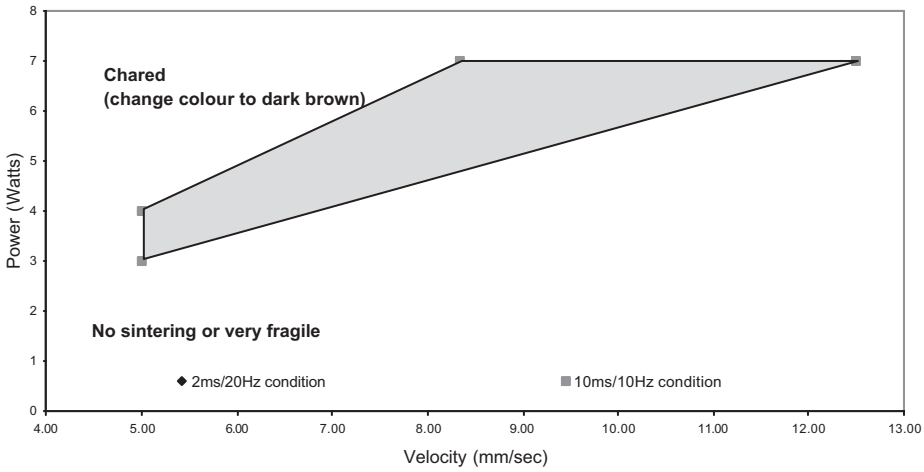

(a)

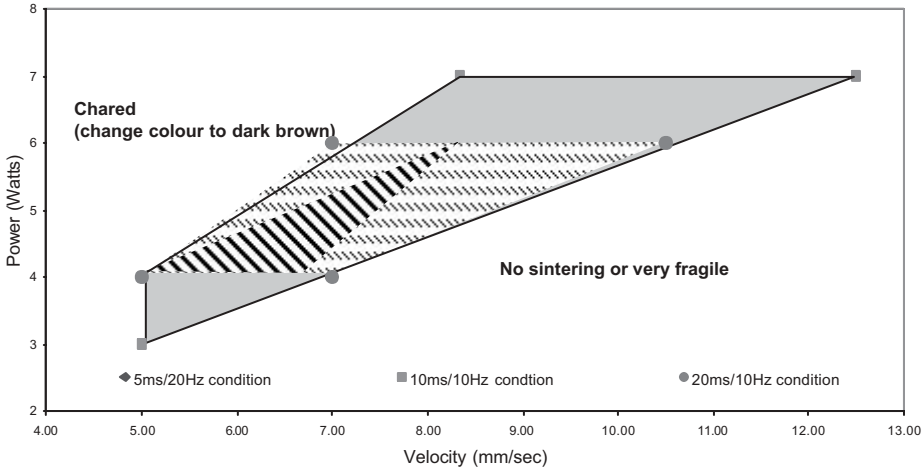

(b)

Fig. 6 Processing window using a Nd:YAG laser; (a) at settings with the same average power and varying peak power; (b) at 5 ms/20 Hz and 10 ms/10 Hz settings with the same average and peak power and 20 ms/10 Hz setting

settings characterized by a low repetition rate and long pulse duration (i.e. 3 Hz and 20 ms), intermediate repetition rate and intermediate pulse duration (i.e. 10 Hz and 10 ms), and high repetition rate and short pulse duration (i.e. 20 Hz and 3 ms) were explored. Table 2 illustrates the peak power ratings at the various parameter settings for an average 4W laser power. It shows that the peak power for the setting (10 Hz and 10 ms) is lower than the other two settings (3 Hz and 20 ms and 20 Hz and 3 ms). Figure 6(a) illustrates that the processing window was the largest at intermediate repetition rate and intermediate pulse duration (i.e. 10 Hz and 10 ms) setting, a smaller number of specimens were fabricated with a high pulse repetition rate and low pulse duration and no acceptable specimens were fabricated by any combination of laser power and scanning speed for setting with low repetition rate and high pulse duration settings. HAPEX® was not sintered at low repetition rate and long pulse duration possibly due to two reasons: first no overlap between consecutive pulses at low repetition rate may have contributed to fragile specimens as a result of weak connections between beads sintered by each pulse; and second, possibly due to the high peak power setting along with a long pulse duration which contributed to specimens that may have been charred, evaporated and/or physically compressed specimens [**20**, **21**]. Evaporation is caused by temperatures well in excess of melt temperature of the powder particles when high peak power is applied.

Table 2 Peak power ratings at various parameter settings for 4 W average power

Parameter setting	Peak power (W)
3 ms/20 Hz	67
10 ms/10 Hz	40
20 ms/3 Hz	67

Only a small number of samples were sintered at high repetition rate and short pulse duration, possibly due to the minimal interaction between the material and the laser pulse, although high peak powers were experienced. A large processing window was observed at intermediate repetition rate and pulse width setting, indicating that some overlap between each pulse, which is determined by repetition rate, and a certain amount of interaction time, which is determined by the pulse width, is favourable for sintering HAPEX®. These results reveal that an appropriate repetition rate and pulse width setting influenced the sintering of HAPEX® even at the same average laser power.

Further investigation of the processing window was carried out by varying the repetition rate and pulse width to obtain consistent peak and average laser power. Three settings were explored: low repetition rate and long pulse duration (5 Hz and 20 ms), intermediate repetition rate and pulse duration (10 Hz and 10 ms), and high repetition rate and short pulse duration (20 Hz and 5 ms). Figure 6(b) illustrates that the processing window is still the largest at intermediate settings. A small window is now observed for high repetition rate and short pulse duration. Compared to the previous test, a slightly longer pulse duration has been used, indicating that a minimum pulse width is required to achieve a certain amount of interaction time to allow the material to sinter. As seen in the previous test, HAPEX® was not sintered at low repetition rate and long pulse duration despite the reduction in peak power, indicating that the repetition rate has to be set to provide a certain overlap between consecutive pulses.

Finally, a test was conducted to observe the effect of a longer interaction time at 10 Hz repetition rate setting by increasing the pulse width to 20 ms. Figure 6(b) illustrates that the processing window is slightly smaller than the processing window observed at settings 10 Hz/10 ms. At low average powers of 3 W, the low peak power of 15 W at 10 Hz/20 ms setting did not generate an acceptable specimen compared to higher peak power of 30 W at 10 Hz/10 ms setting. At the same average power, the peak power for the larger pulse width of 20 ms is much lower than that of pulse width 10 ms. It was observed that HAPEX® particles did not sinter at low powers of 3 W, possibly due to low peak power values of 15 W and fragile specimens. At a power 7 W at velocities above 8 mm/s this behaviour still cannot be understood fully. However, it is possibly due to the combined effects from various factors including peak power, energy density, and no overlap that a transition was experienced. Moreover, it was observed that the fragile specimens built at 7 W above 8 mm/s had a larger bead width than the spot diameter. This is possibly due to the longer interaction time. This trend has been observed by other materials such as tool steel [**22**].

From the above set of tests it is quite obvious that the repetition rate and pulse width are two factors which affect pulse overlap, interaction time, and peak power and therefore affect the processing window of HAPEX®.

3.3 Effect of particle size on the processing window

When a laser scans over the powder bed, the laser energy is directly absorbed by the powder particles. It is known that a greater surface–volume ratio of finer powders leads to higher amounts of laser energy absorption, thereby increasing the temperature and sintering kinetics [**23**]. It was found that this phenomenon is applicable to both the CO_2 and the Nd:YAG lasers. Figures 5 and 6 illustrate the effect of particle size on the operation window. A single processing window was obtained for <75 μm, 75–106 μm, and 106–150 μm particles on the CO_2 laser system and <75 μm and 75–106 μm on the Nd:YAG laser system. However, a shift in the CO_2 process window to higher energy density for sintering particles in the range of 150–212 μm was exhibited (see Fig. 5). Larger particles required a higher energy density ranging between 0.15 J/mm^2 to 0.3 J/mm^2 for sintering to occur. This was possibly due to the reduced surface–volume ratio, which tends to reduce the kinetics of densification. The result is similar to the previous study by Simchi with iron powders in which finer particles need less energy due to the enhancement of densification kinetics [**23**].

The effect of HAPEX® particle size is greater on the Nd:YAG laser system as compared to the CO_2 laser system. The Nd:YAG laser system processed particles up to 106 μm, whereas the CO_2 laser processed powders up to a range of 212 μm. This was possibly due to the interaction between the different lasers and material. Due to the higher adsorption of laser power by particles on the CO_2 laser, the CO_2 laser would better induce the melting at the surface of the particles and allow greater bonding between the particles and the sintering of larger particles.

3.4 Layer sintering by CO_2 and Nd:YAG laser

3.4.1 Effect of CO_2 and Nd:YAG laser on layer sintering

Figures 7 and 8 illustrate the sintered surfaces of the single-layered specimens built with CO_2 and Nd:YAG lasers. The manner in which particle fusion took place between particles differed by varying the laser source. A larger amount of contact necking between

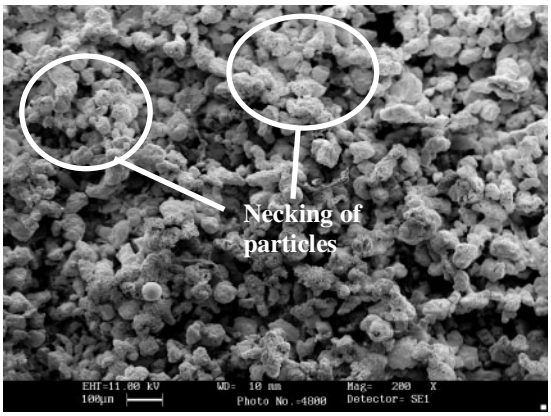

(a)

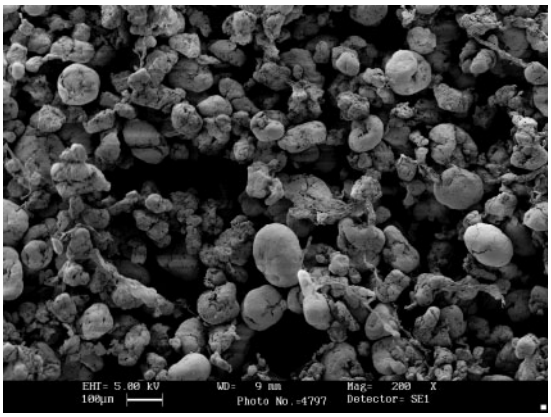

(b)

Fig. 7 SEM micrograph of sintered single layers with particle size (a) <75 μm, (b) 75–106 μm using a CO_2 laser 2 W, 1000 mm/s

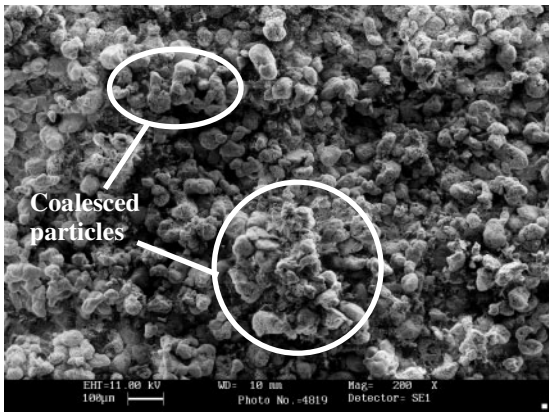

(a)

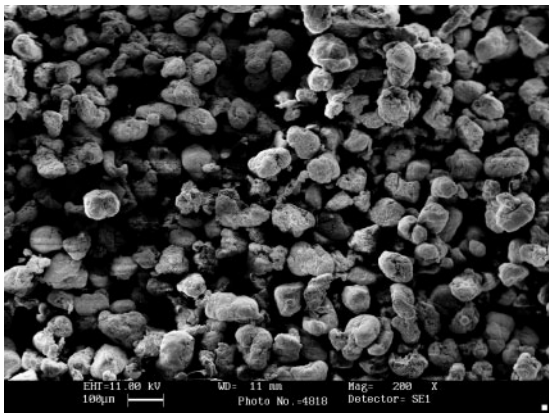

(b)

Fig. 8 SEM micrograp of sintered single layers with particle size (a) <75 μm; (b) 75–106 μm using a Nd:YAG laser 3 W, 5 mm/s

particles was observed for layers sintered by the CO_2 laser as shown in Fig. 7. However, a few incidences of contact necking between particles on the surface of the specimen sintered by the Nd:YAG source were observed with a large number of particles coalesced to form larger single structures. These results reveal that the particles melting existed in both laser sintering processes, although different extents occurred in both CO_2 and Nd:YAG laser sintering. The Nd:YAG laser was operated at the low scanning velocity of 5 mm/s, and scanned the powder 200 times slower than the CO_2 laser operated at 1 000 mm/s. Therefore, the duration time of the particles melting (liquid phase sintering) is different between the CO_2 and Nd:YAG laser sintering. The amount of binding is a function of time and dictates the amount of material rearrangement (melting and capillary penetration) during selective laser sintering [**5**]. For CO_2 laser sintering, the liquid phase sintering of the particles was most possibly in the early stage. However, the melt did not flow due to the short duration time. It could also be that the later stages of liquid phase sintering occurred in the particles following Nd:YAG processing and therefore surface tension-driven melt displacement drove the molten volume such that adjacent particles bonded and formed the dense conglomerated structure.

Figures 7(b) and 8(b) illustrate that particle bonding seems to be greater on specimens sintered using a CO_2 laser as compared to the Nd:YAG laser for particles between 75 and 106 μm. However, contact points between particles or necking between particles are not visible for either specimen.

3.4.2 *Effect of particle size on CO_2 and Nd:YAG layer sintering*

The effect of particle size on layer sintering was observed through SEM images. Figures 8(a) and (b) illustrate that layered structures sintered from particles <75 μm coalesced, possibly by later stages of liquid phase sintering, to form larger structures using a Nd:YAG laser. However, this form or any form of sintering is not visible in larger particles between 75 and 106 μm. Figures 7(a) and (b) illustrate that particles below 75 μm experience a larger amount of necking between particles as compared to particles of size 75–106 μm using a CO_2 laser.

These results clearly show that particle binding reduces significantly with an increase in particle size. This is supported by the concept of finer particles enhancing kinetics of densification [**20**].

3.4.3 *Sintering depth and true density of CO_2 and Nd:YAG sintered layers*

When building a three-dimensional multi-layer part, the induced energy should be able to penetrate the powder deep enough to bind the different layers properly together. The layer thickness is measured as an indication of the penetration depth of the laser energy.

Figures 9 and 10 illustrate that energy density has a significant effect on the sintering depth or layer thickness and weight of the sample. As the energy density increased the layer thickness and weight of the part increased for both the CO_2 and the Nd:YAG laser. This may be because the higher energy density imparted more energy into the unit powder area and generated a high degree of melting and bonding between the particles, which induced the fusion of more particles and produced a greater sintering depth. The results showed that the samples made with the Nd:YAG laser were much thicker than those made with the CO_2 laser. This may have been due to the energy density used for Nd:YAG laser sintering being much higher than that used for CO_2 laser sintering.

The true density of a part is the fraction of weight and volume of a sintered layer. Figures 11 and 12 illustrate that energy density values influence the true density of layer-sintered parts. However, it was found that the relationship between energy density and true density is not linear. This may possibly be due to the inconsistent variation in the proportional decrease of layer thickness and specimen weight with respect to the energy density values as shown in Figs 9 and 11. It was also observed that the density values for specimens sintered by the Nd:YAG laser were higher than specimens sintered using a CO_2 laser. This may have been because the duration time of Nd:YAG sintering was longer than that of

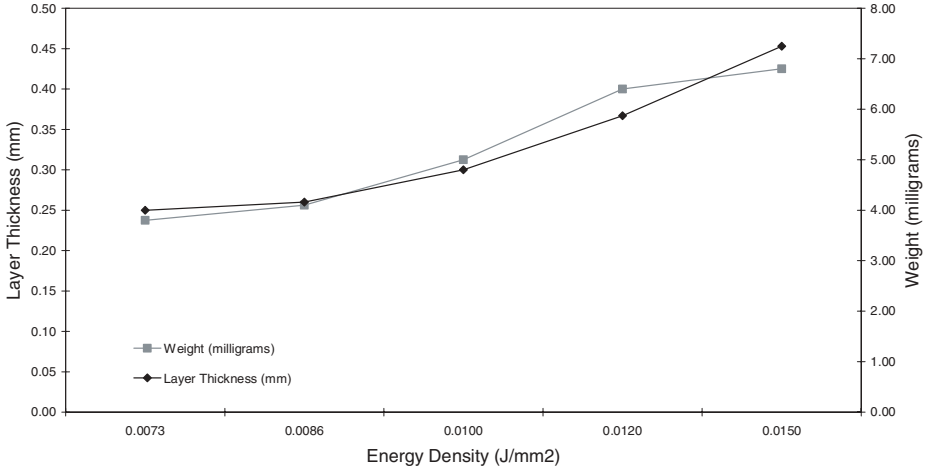

Fig. 9 Layer thickness and weight of single-layered specimens using a CO_2 laser

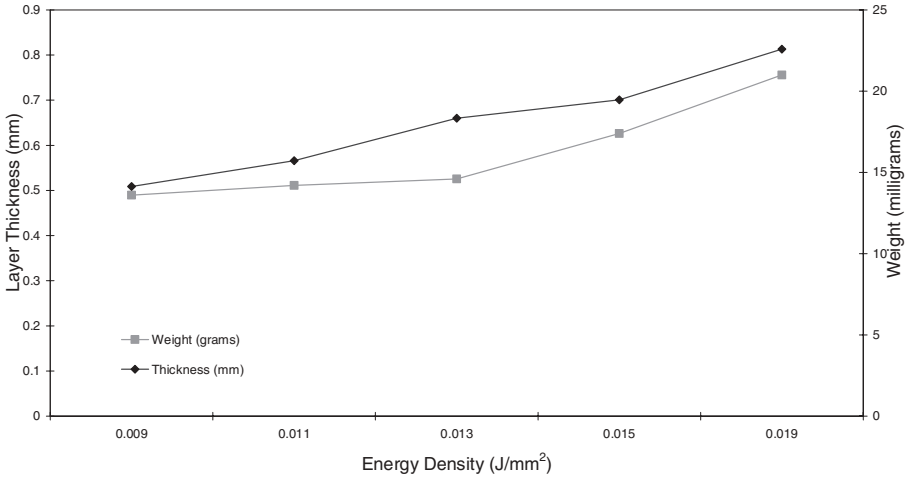

Fig. 10 Layer thickness and weight of single-layered specimens using a Nd:YAG laser

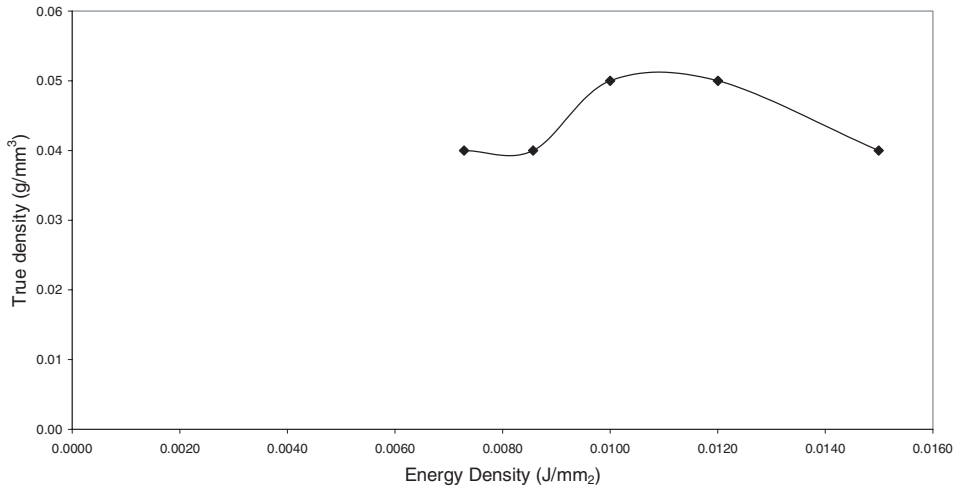

Fig. 11 True density of samples sintered at various energy densities using a CO_2 laser

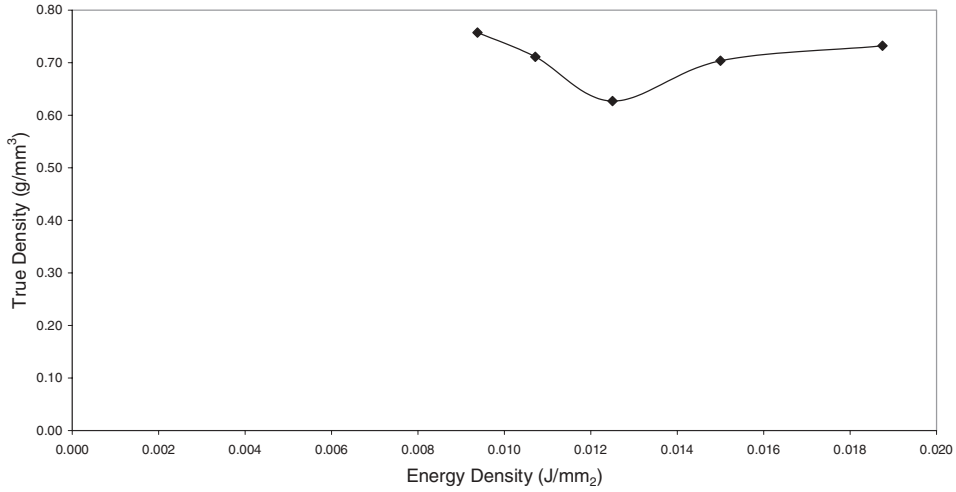

Fig. 12 True density of samples sintered at various energy densities using a Nd:YAG laser

CO_2 laser sintering which allowed the higher degree of particle bonding and densification.

4 CONCLUSION

This study presents the performance and feasibility of the CO_2 laser and Nd:YAG laser for the sintering of commercial-grade HAPEX® composite.

Acceptable specimens could be sintered by a CO_2 laser using a large range of laser powers and scanning speeds. The Nd:YAG laser was also able to sinter acceptable specimens. Furthermore, the operation window of the Nd:YAG laser sintering was dependent on the pulse duration and pulse repetition rate. The most effective window was found at intermediate pulse duration and pulse rate. Compared to the Nd:YAG laser, the CO_2 laser has a larger operation window and presents better controllability for SLS of the material.

It was found that particle size had a significant effect on the sintering of HAPEX®. The Nd:YAG laser could sinter particles up to 106 μm whereas particles up to 212 μm could be sintered on the CO_2 laser. Furthermore, the binding mechanisms between particles sintered using a Nd:YAG laser and a CO_2 laser differed. Necking was extremely evident between particles sintered using the CO_2 laser while the formation of coalesced particles was more evident using the Nd:YAG laser. Therefore, compared to the Nd:YAG laser, the CO_2 laser is capable of processing a larger range of particles sizes and providing more evidence of particle necking.

The processing energy density range for the CO_2 laser system fell between 0.01 and 0.02 J/mm^2 while the energy density required by the Nd:YAG laser was approximately 1 J/mm^2, indicating that the CO_2 laser has a better processing efficiency than the Nd:YAG laser for sintering HAPEX® composite. In addition, the CO_2 laser can be operated at higher scanning speeds and would therefore possess a greater manufacturing speed.

Compared to the Nd:YAG laser specimens, the CO_2 aser specimens yielded a lower density. For the laser sintering of traditional materials such as metal, lower density would be considered as a disadvantage in terms of mechanical properties. However, the lower density (high porosity) would be a useful feature for HAPEX® composites, allowing them to be used as specialized implants and tissue scaffolds. Therefore, it has been demonstrated that a CO_2 laser system has better potential to fabricate porous HAPEX® products than a Nd:YAG laser system.

ACKNOWLEDGEMENTS

The authors would like to express their gratitude to Dr Y. Zhang and Prof. K. E. Tanner at Queens Mary University of London for providing the HA-HDPE materials and the UK Department of Health's New and Emerging Applications of Technology (NEAT E059) for providing financial support.

REFERENCES

1 **Kruth, J. P., Leu, M. C.,** and **Nakagawa, T.** Progress in additive manufacturing and rapid prototyping. *Ann. CIRP*, 1998; pp. 525–540.

2 **Gill, T. J.** and **Hon, K. K. B.** Experimental investigation into the selective laser sintering of silicon carbide polyamide composites. *Proc. Instn Mech. Engrs, Part B: J. Engineering Manufacture*, 2004, **218,** 1249–1256.

3 **Leong, K. F., Phua, K. K. S., Chua, C. K., Du, Z. H.,** and **Teo, K. O. M.** Fabrication of porous polymeric matrix drug delivery devices using the selective laser sintering technique. *Proc. Instn Mech. Engrs, Part H: J. Engineering in Medicine*, 2001, **215**(H2), 191–201.

4 **Williams, J. D.** and **Deckard, C. R.** Advances in modelling the effects of selected parameters on the SLS process. *Rapid Prototyping J.*, 1998, **4**(2) 90–100.

5 **Kruth, J. P., Mercelis, P.,** and **Vaerenbergh, J. V.** Binding mechanisms in selective laser sintering and selective laser melting. *Rapid Prototyping J.*, 2005, **11**(1), 26–36.

6 **Kruth, J. P., Wang, X., Laoui, T.,** and **Froyen, L.** Lasers and materials in selective laser sintering. *Rapid Prototyping J.*, 2003, **23**(4), 357–371.

7 **Tolochko, N. K., Laoui, T., Khlopkov, Y. V., Mozzharouv, S. E., Titov, V. I.,** and **Ignatiev, M. B.** Absorptance of powder materials suitable for laser sintering. *Rapid Prototyping J.*, 2000, **6**(3), 155–160.

8 **Steen, W. M.** In *Laser material processing*. 1998, p. 47 (Springer Verlag).

9 **Vaucher, S., Paraschivescu, D., Andre, C.,** and **Beffort, O.** Selective laser sintering of aluminium-silicon carbide metal matrix composites. In *Materials Week*, 2002.

10 **Bourell, D. L., Marcus, H. L.,** and **Barlow, J. W.** Selective laser sintering of metals and ceramics. *Int. J. Powder Metal.*, 1992, **28**(4), 369–381.

11 **Alexandre, T., Giovanola, J., Vaucher, S., Beffort, O.,** and **Vogt, U.** Layered manufacturing of porous ceramic parts from SIC powders and preceramics polymers. *Laser Assisted Net Shape Engng.*, 2004, **4**, 497–506.

12 **Kruth, J. P., Peeters, P., Smolderen, T., Bonse, J., Laoui, T.,** and **Froyen, L.** Comparison bewteen CO2 and Nd: YAG lasers for use with selective laser sintering of steel-copper powders. *Int. J. CADCAM and Computer Graphics*, 1998, **13**(4–6), 95–110.

13 **Tan, K. H., Chua, C. K., Leong, K. F., Cheah, C. M., Cheang, P., Abu Bakar, M. S.,** and **Cha, S. W.** Scaffold development using selective laser sintering of polyetheretherketone-hydroxyapatite biocomposite blends. *Biomaterials*, 2003, **24**(18), 3115–3123.

14 **Chua, C. K., Leong, K. F., Wiria, F. E., Tan, K. C.,** and **Chandrasekara, M.** Fabrication of poly(vinyl alcohol)/hydroxyapatite in tissue engineering. International conference on *Competitive manufacturing*, 2004.

15 **Bonfield, W., Behiri, J. C., Doyle, C., Bowman, J.,** and **Abram, J.** Hydroxyapatite reinforced polyethylene composites as analogous bone replacement materials. *Biomaterials '84:* Second world congress on *Biomaterials,* 10th annual meeting of the society for biomaterials, sixteenth international biomaterials symposium. 1984. Washington DC, USA.

16 **Bonfield, W., Doyle, C.,** and **Tanner, K. E.** In vivo evaluation of hydroxyapatite reinforced polyethylene composites. In Biological and Biomechanical performance of biomaterials, proceedings of the fifth European confererence on *Biomaterials*. 1986. Paris, France.

17 **Eniwumide, J. O., Joseph, R.,** and **Tanner, K. E.** Effect of particle morphology and polyethylene molecular weight on the fracture toughness of hydroxyapatite reinforced polyethylene composite. *J. Mater. Sci: Mater. Med.*, 2004, **15**(10), 1147–1152.

18 **Ladizesky, N. H., Wang, M., Miettinen, E. M., Tanner, K. E., Ward, I. M.,** and **Bonfield, W.** Hydrostatic extrusion of hydroxyapatite polyethylene composite. In Fifth World Biomaterials Congress. 1996. Toronto, Canada.

19 **Wang, M., Porter, D.,** and **Bonfield, W.** Processing, characterisation, and evaluation of hydroxyapatite reinforced polyethylene composites. *Br. Ceramic Trans.*, 1994, **93**, 91–95.

20 **Morgan, R., Sutcliffe, C. J.,** and **O'Neill, W.** Experimental investigation of nanosecond pulsed Nd: YAG laser re-melted pre-placed powder beds. *Rapid Prototyping J.*, 2001, **7**(3), 159–172.

21 **Kruth, J. P., Froyen, L., Vaerenbergh, J. V., Mercelis, P., Rombouts, M.,** and **Lauwers, B.** Selective laser melting of iron-based powder. *J. Mater Process. Technol.*, 2004, **149**, 616–622.

22 **Su, W. N., Erasenthiran, P.,** and **Dickens, P. M.** Investigation of fully dense laser sintering of tool steel powder using a pulsed Nd: YAG laser. *Proc. Instn Mech. Engrs, Part C: J. Mechanical Engineering Science*, 2002, **217**(C), 127–138.

23 **Simchi, A.** The role of particle size on the laser sintering of iron powder. Metall. Mater. Trans. B, 2004, **35**(B), 937–948.